Original paper Non-invasive characterization of coronary artery atherosclerotic plaque using dual energy CT: Explanation in ex-vivo samples

Article *in* Physica Medica · August 2020

CITATION
1

READS
153

12 authors, including:

Avinav Bharati
Bhabha Atomic Research Centre
44 PUBLICATIONS **52** CITATIONS
SEE PROFILE

Rezvan Ravanfar Haghighi
Shiraz University of Medical Sciences
9 PUBLICATIONS **3** CITATIONS
SEE PROFILE

Priya Jagia
All India Institute of Medical Sciences DELHI
207 PUBLICATIONS **1,400** CITATIONS
SEE PROFILE

Sanjiv Sharma
All India Institute of Medical Sciences
26 PUBLICATIONS **112** CITATIONS
SEE PROFILE

Physica Medica 45 (2018) 52–58

Contents lists available at ScienceDirect

Physica Medica

journal homepage: www.elsevier.com/locate/ejmp

Original paper

Non-invasive characterization of coronary artery atherosclerotic plaque using dual energy CT: Explanation in ex-vivo samples

Susama Rani Mandal[a], Avinav Bharati[a], Rezvan Ravanfar Haghighi[b], Sudhir Arava[c], Ruma Ray[c], Priya Jagia[d], Sanjiv Sharma[d], Sabyasachi Chatterjee[e], Millo Tabin[f], Munish Sharma[f], Sanjay Sharma[g], Pratik Kumar[a,*]

[a] Medical Physics Unit, Dr. B.R.A. Institute Rotary Cancer Hospital (IRCH), All India Institute of Medical Sciences (AIIMS), New Delhi 110029, India
[b] Medical Imaging Research Center, Shiraz University of Medical Sciences, Shiraz, Iran
[c] Department of Cardiac Pathology, AIIMS, New Delhi 110029, India
[d] Department of Cardiac Radiology, AIIMS, New Delhi 110029, India
[e] BGVS, Chemical Engineering Building (Old), Indian Institute of Science Campus, Bangalore 560012., India
[f] Department of Forensic Medicine, AIIMS, New Delhi 110029, India
[g] Department of Radiology, AIIMS, New Delhi 110029, India

ARTICLE INFO

Keywords:
Non-invasive
Dual energy CT
Atherosclerosis
Compositional analysis

ABSTRACT

Purpose: In this study non-calcified plaque composition is evaluated by Dual Energy CT (DECT). Energy Dispersive X-ray Spectroscopy (EDS) has been used to study the Plaque composition. An attempt has been made to explain the DECT results with EDS analysis.

Methods: Thirty-two ex-vivo human cadaver coronary artery samples were scanned by DECT and data was evaluated to calculate their effective atomic number and electron density (Z_{eff} & ρ_e) by inversion method. Result of DECT was compared with pathology to assess their differentiating capability. The EDS study was used to explain DECT outcome.

Results: DECT study was able to differentiate vulnerable plaque from stable with 87% accuracy (area under the curve (AUC):0.85 [95% confidence interval {CI}:0.73–0.98}] and Kappa Coefficient (KC):0.75 with respect to pathology. EDS revealed significant compositional difference in vulnerable and stable plaque at $p < .05$. The weight percentage of higher atomic number elements like F, Na, Mg, S, Si, P, Cl, K and Ca was found to be slightly more in vulnerable plaques as compared to a stable plaque. EDS also revealed a significantly increased weight percentage of nitrogen in stable plaques.

Conclusions: The EDS results were able to explain the outcomes of DECT study. This study conclusively explains the physics of DECT as a tool to assess the nature of non-calcified plaques as vulnerable and stable. The method proposed in this study allows for differentiation between vulnerable and stable plaque using DECT.

1. Introduction

Atherosclerosis is characterized by intracellular and extracellular deposition of lipid and its derivatives in the subintimal layer of the arteries [1]. One of the common complications of atherosclerotic plaque is embolization which depends on the vulnerability of the plaque. A calcified plaque is vulnerable by nature [2,3] while a non-calcified plaque can be vulnerable when it shows high extracellular lipid, thin fibrous cap, surface ulceration and hemorrhage [2]. A non-calcified plaque may be vulnerable or stable depending upon the composition of plaque.

Various non-invasive imaging like ultrasound, MRI and CT angiography though may differentiate calcified and non-calcified plaque [4] but have proved to be inadequate to determine the nature of non-calcified plaque. A non-calcified plaque may be vulnerable or stable depending upon its composition. A vulnerable non-calcified plaque has a lipid rich core overlying with a thin fibrous cap ($< 65\,\mu m$) whereas a stable non-calcified plaque may either be fibrous or of intermediate fibro-lipid composition (with $> 65\,\mu m$ thickness of fibrous cap) [2,3,5]. It is to be noted that spatial resolution of modern CT system is limited (range of mm) and does not allow detecting objects of about $65\,\mu m$. Although, CT angiography identifies low-attenuation areas of plaque, more precise identification requires better discrimination of lipid core and fibrous cap which is compromised due to

* Corresponding author.
E-mail address: drpratikkumar@gmail.com (P. Kumar).

https://doi.org/10.1016/j.ejmp.2017.12.006
Received 31 March 2017; Received in revised form 3 December 2017; Accepted 4 December 2017

their similar X-ray attenuation and thus overlapping Hounsfield Unit (HU) or CT numbers [6–13]. Even an advanced imaging method like Dual Energy CT (DECT) gives overlapping HU values for similar tissues [13–15]. Phantom study have shown that coronary artery with stenosis is more susceptible to variation in HU values due to factors like CT scanner speed, scanning method and scan time after contrast medium injection [16]. Moreover, HU values are machine dependent parameter which means they vary with source spectrum, detector efficiency, filter configuration of CT machine leading to difficulty in characterizing vulnerable and stable plaques.

X-ray attenuation and hence HU values of scanned material depends upon the energy of incoming photons and also on Z_{eff} & ρ_e of the material. Thus from HU values Z_{eff} & ρ_e of the material may be calculated. DECT records two HU values at a point, simultaneously, at two different voltages. These two HU values have been used to get material specific information by Inversion method [17,18] established by us. These material specific informations were electron density (ρ_e) and effective atomic number (Z_{eff}) of non-calcified atherosclerotic plaque [17]. The attenuation coefficients (HU values) obtained in DECT is sensitive to variation in composition of scanned tissues [19]. The present study has attempted to compare vulnerable and stable plaques based upon their Z_{eff} and ρ_e values obtained from DECT inversion. These results were compared to reference standard histopathology to assess its differentiation capability. However, pathological studies do not give chemical specific information which is needed to explain the difference in Z_{eff} values of plaques obtained by DECT inversion. For this, Scanning Electron Microscopy (SEM) and Energy Dispersive X-ray spectroscopy (EDS) chemical analysis were carried out which validated and explained the DECT outcomes.

2. Materials and methods

2.1. DECT study

2.1.1. Sample acquisition

Fifty-five excised human left coronary artery samples were collected from autopsy hearts of all age groups after the approval from Medical Ethics Committee of AIIMS. Proper consent from a relative or legal representative of the deceased was obtained.

Left Anterior Descending (LAD) coronary artery along with adjacent cardiac muscles (to keep the vessel in normal anatomical position) was dissected from its origin till the end (up to the apex of the heart with an average length of 10 cm). The excised LAD samples were immediately placed in 0.9% normal saline and kept in a refrigerator at 4 °C. The autopsy samples of LAD were collected from people who died due to Coronary Artery Diseases (CAD) and also from people (with no known CAD issues) who died due to road traffic accident, fall from height, alcohol intoxication, and suicide. The details of deceased were collected from the medical records.

2.1.2. DECT scanning

Samples were removed from saline just before the DECT scan and were injected with a viscous form of iodinated contrast material [18,20] into the LAD lumen. DECT scans were performed by placing the coronary artery ostium in the cranial position and the rest of the full-length of the samples was aligned along with the z-axis of the couch (Fig. 1a). All scans were performed on Dual Source CT SOMATOM Definition (Siemens AG, Germany) by using Perfusion Blood Volume (PBV) protocol. This protocol used 100 and 140 kVp, electrocardiographic gating (which gives a demo ECG of 60 beats/min), 64 × 0.6 mm collimation, 83 ms temporal resolution, pitch of 0.25 and rotation time 330 ms. Reconstructed images were obtained from 0.6 mm thick slice, B26f convolution kernel, and 512 × 512 matrix size. Maximum intensity projection mode was used to evaluate the presence of non-calcified plaque in the LAD and the distance between coronary ostium to the plaque was measured (Fig. 1b). Also, any landmarks such as the origin of side branches and their distances from the target plaque were noted down. This measured distance was used as a marker for macroscopic evaluation for the presence of plaque and multiple sections of about 3 mm along the length of the plaque were dissected. Representative sections were submitted to cardiac-pathologist for analysis. From these sections very thin superficial sections were cut for SEM-EDS analysis. Scanned CT data were transferred to the multi-modality workstation for post-scan data processing.

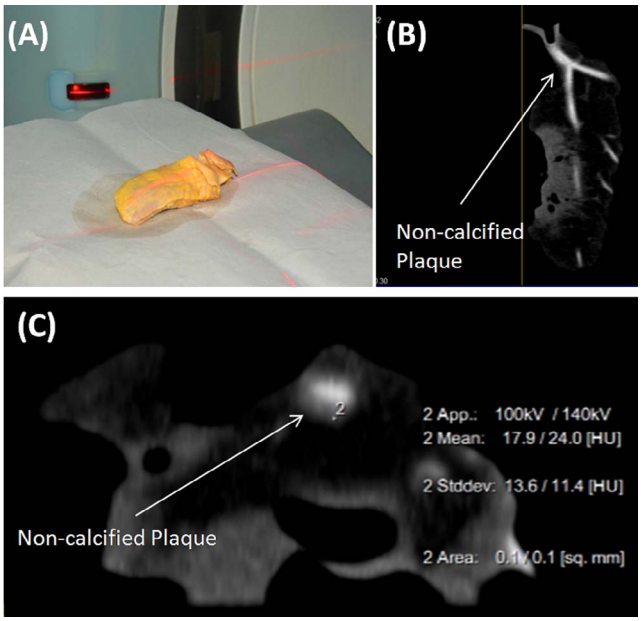

Fig. 1. (a) Section of heart containing LAD, positioned on the scanning table. (b) Typical MIP image of LAD containing soft plaque in proximal part. (c) Corresponding true axial image to read HU values.

2.1.3. Post scan processing

Images were oriented to get the true axial image of plaque (Fig. 1c). To read the HU values, circular region of interest (ROI) were selected in the axial slices along the length of the plaque starting from the first till the last axial slice of plaque.

These ROI (0.1–0.3 mm^2) were placed at the centre of plaque area in axial slices in such a ways that at least each ROI must contain three pixels (3 pixel per ROI) so that HU values can be statistically accepted. Also, ROI dimension must not exceed 0.3 mm^2 so that contamination due to neighbouring structures (wall, soft tissue, and contrast in lumen) can be avoided. Data was recorded three times (i.e. 3 ROI/axial slice) in an axial slice along the length of the plaque for the same plaque. This process was repeated for all the plaque samples.

2.1.4. DECT inversion

We have used MATLAB; R2015b software (Mathworks, Natick, MA) for all numerical calculation. The HU values of plaques were subjected to a method called inversion algorithm developed by our group [18]. In present paper we further improvised our algorithm which established the relation of Z_{eff} and ρ_e with the HU of the object scanned at 100 and 140 kVp also called HU(100) and HU(140).

$$Z_{eff} = \left[\frac{(\chi(100,140) - a_1)}{b_1}\right]^{\frac{1}{X}} \quad \text{or } b_1 Z_{eff}^{X} + a_1 = \chi(100,140) \tag{1}$$

where,

$$\chi(100,140) = \frac{HU(100) - HU(140)}{HU(100) + HU(140)} \tag{2}$$

Here, the functional form of χ(100,140) maximizes the difference in attenuation at 100 & 140kVp compared to ratio HU(100)/HU(140)

used previously.

$$\rho_e = F(V)/(a_2 + b_2 Z_{eff}^x) \quad (3)$$

where, $F(V) = [HU(V)/1000 + 1]$ and "V" represents the excitation voltage 100 or 140 kVp for which we have license from the manufacturer. Simplifying Eq. 3 further in this study by taking log and using approximation, $b_2/a_2 \ll 1$ equation becomes

$$\log(\rho_e) - \log(F(V)) = a_2 + b_2 Z_{eff}^x \quad (4)$$

By knowing $\chi(100,140)$ and F(V) we can determined Z_{eff}^x and ρ_e. Finally Z_{eff} can be found as,

$$Z_{eff} = 10^{a_3} z_{eff}^{xb_3} \quad \text{Or} \log(Z_{eff}) = a_3 + b_3 \log(Z_{eff}^x) \quad (5)$$

As is understood, the values of the coefficient a_1, b_1, a_2, b_2, a_3, and b_3 ought to be known in order that the above inversion procedure can be applied. This has to be done with an independent set of experiments. The coefficients a_1, b_1, a_2, b_2, a_3, and b_3 were obtained by scanning different known chemical compounds like Acetone, Diethyl Glycol, and Diethyl ether in addition to all compounds previously [18] used by the DECT to get their HU values at 100 and 140 kVp. Adding these additional chemicals expanded the range of the atomic number of the calibration imparting the inversion algorithm further improvement. For all these compounds exponent X, Z_{eff} and ρ_e were theoretically calculated [17]. Thereafter, these values of Z_{eff}, ρ_e, exponent X and HU values were substituted in Eqs, 1, 4 and 5 and solved to obtain the values of the coefficients a_1, b_1, a_2, b_2, a_3, and b_3. Finally HU values of the plaque along with these coefficients can be substituted in above equations to get Z_{eff} and ρ_e of plaques which is the purpose of the inversion method.

2.2. Sample preparation for pathology

Representative plaque sections were placed in 10% buffered formalin solution for pathological analysis. Paraffin blocks were prepared by processing the sample in automated histokinetic processor. Sections with a thickness of 5-μm sections were cut and stained with routine hematoxylin and eosin for a definitive diagnosis. In pathology, reports plaques were identified as vulnerable and stable based on the thickness of fibrous cap, large extracellular lipid, and hemorrhage by two experienced cardiovascular pathologists who were blinded to the outcome of the DECT.

2.3. Sample preparation for Scanning Electron Microscope-Energy Dispersive X-ray Spectroscopy

SEM-EDS preserve the tissue architecture during the analysis and have better resolution than optical microscope prompting us to select it as the confirmatory tool for characterization of plaques. Very thin sections from plaque samples were taken and prepared by using standard protocol [21]. These sections were dried at ambient atmosphere for 24–48 h depending on weather condition. The dried samples were mounted on Aluminum stub using carbon tape and coated with platinum (35 mA for 120 s) using Quorum Q150RES coater to avoid charge accumulation on the surface of the samples which makes a pathway to the ground. These samples were then loaded in machine Zeiss supra 55 (Carl Ziess supra, Germany). Fig. 2 illustrates a plaque section with marked locations "A, B, C, D" were EDS observations were taken. Similarly, EDS analysis was undertaken for all samples.

3. Results

In our study, the mean age of the deceased subjects was 39 years (max. 55 years and min 23 years) with a sex ratio of 3:52 (Female: Male). The mean plaque size was 1.95 ± 0.84 cm. From DECT images it was found that 32 out of 55 samples had non-calcified atherosclerotic plaque. Rest 23 samples were excluded from the study as 10 samples did not have plaque and 13 samples showed calcified plaques. These excluded samples were returned to the morgue for their proper disposal. Therefore, final study group consisted of total 32 non-calcified plaque samples.

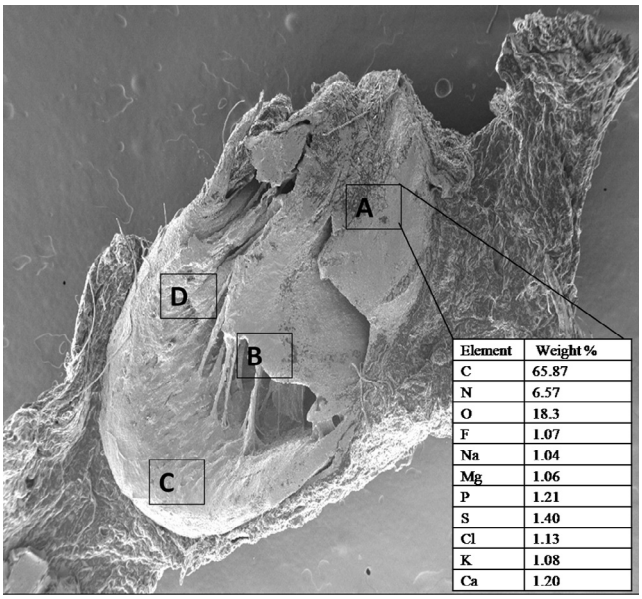

Fig. 2. Scanning Electron Micrographs of a sample showing EDS analysis done at marked regions A, B, C, & D. Inserts shows the table indicating various elements at region A.

3.1. Pathology report

Out of 32 samples, pathological examination revealed 18 samples as vulnerable and 14 as stable atherosclerotic plaques. Fig. 3 illustrate gross images and the corresponding view under the light microscope for a vulnerable and stable sample.

3.2. DECT inversion results

The values of coefficients (a_1, b_1), (a_2, b_2), (a_3, and b_3) are found from the corresponding linear regression fit of inversion Eqs. 1, 4 and 5 respectively. These values were marginally different from previously reported [18] values because of the improvisation made in this paper for the same CT machine that was used and were found to be $a_1 = 195.13$, $b_1 = 8.2127 \times 10^3$, $a_2 = -0.5424$, $b_2 = 1.6338 \times 10^{-4}$, $a_3 = 1.6344$, and $b_3 = 0.2923$. The calibration gives Z_{eff} within ± 1% and the ρ_e within ± 3.5% of known values with 95% confidence for all the chemical sample chosen for calibration which is considered to be acceptable [18]. Applying inversion algorithm to all 32 plaque samples revealed Z_{eff} to lie in the range 6 to 8.5 which is our range of interest and ρ_e within the range of 3 to 4 ($\times 10^{23}$ per cc) (shown in Fig. 4).

3.3. Statistical analysis

The Z_{eff} and ρ_e values of plaques were compared with histopathology and Receiver Operating Characteristic (ROC) curve analysis [22] was performed. ROC analysis on Z_{eff} indicated 7.4 as the threshold with 95% sensitivity to discriminate vulnerable versus stable plaque. The scatter plot of Z_{eff} versus ρ_e for all the plaque samples revealed two distinct regions "I, and II" as shown in Fig. 4. Region "I" has $Z_{eff} < 7.4$ and region "II" has $Z_{eff} > 7.4$. Subsequently, the ratio of the number of points in region "I" to the number of points in region "II" was calculated for all the samples. This ratio was called Distribution Index (DI) and ROC analysis was carried out on DI values. The cut-off value of "DI" was found to be ≤0.08 to categorize plaque as vulnerable with 85% accuracy {area under the ROC curve [AUC]: 0.85 [95% confidence interval

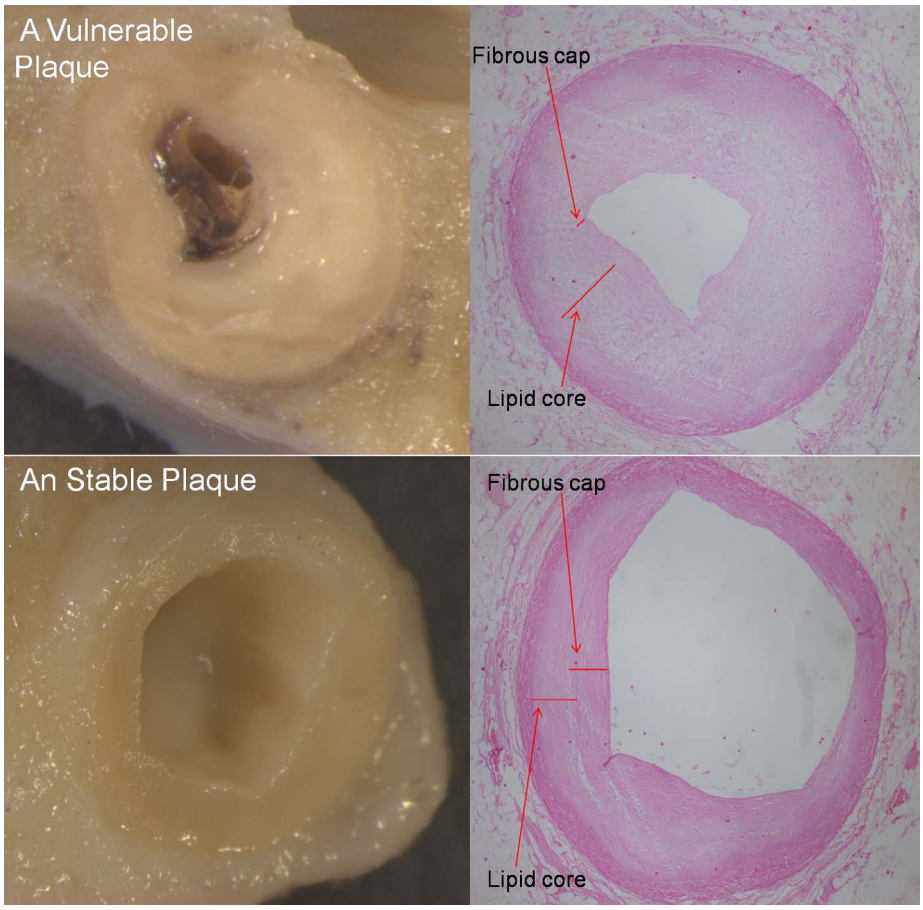

Fig. 3. Gross image of atherosclerotic plaques and corresponding microscopic view.

(CI): 0.73–0.98]} with kappa coefficient (KC:0.75). DI values of ≤ 0.08 implies that only 8% of the data points (z_{eff}, ρ_e) lie in region I (Fig. 4) and rest 92% of data points lie in region II for a plaque sample. In other words, if total n ROIs were recorded for a sample then ≤8% of these n ROIs lie in region I ($z_{eff} < 7.4$). DECT inversion based categorization of plaque compared to pathology and corresponding statistical results [Sensitivity (Sn), Specificity (Sp), Positive predictive value (PPV), Negative predictive value (NPV), Accuracy (ACC) and kappa coefficient (KC)] have been tabulated in Table 1 which suggests our scheme of classification to be highly effective. We find that 16 plaque samples were categorized as vulnerable and 16 plaque samples were categorized as stable.

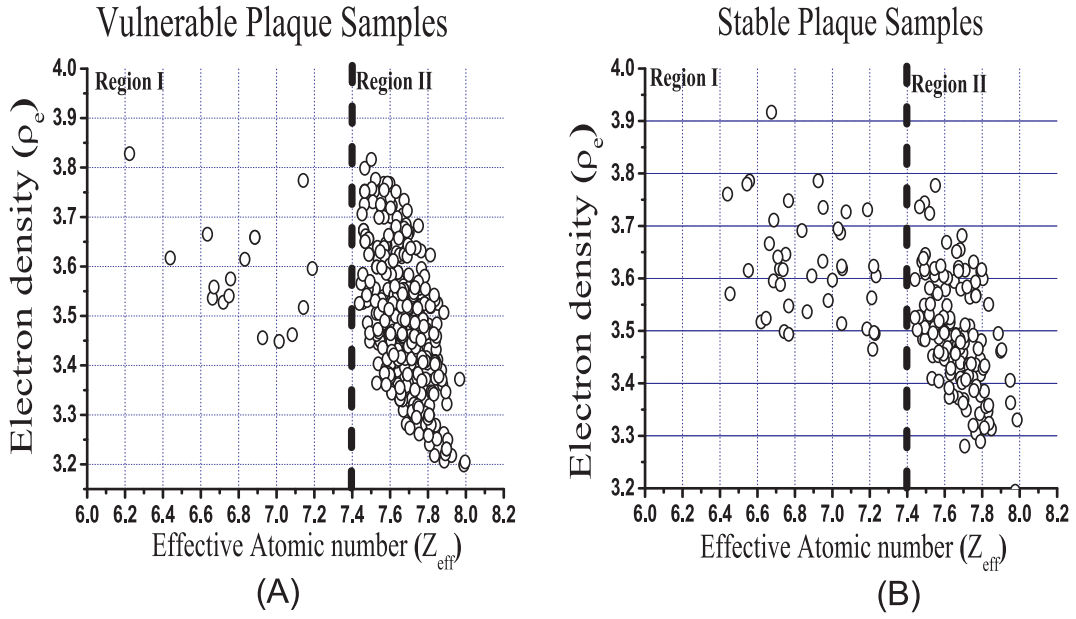

Fig. 4. Z_{eff} versus ρ_e plot with region I and II, (a) combined plot of 18 pathologically vulnerable plaques. (b) Combined plot of 14 pathologically defined stable plaques.

Table 1
Comparison of results of pathology and DECT inversion and corresponding statistical results of correlation (total number of samples = 32).

DECT[a] inversion based differentiation	Pathology based differentiation		Statistical results of correlation
	Vulnerable samples (18)	Stable samples (14)	
Vulnerable samples (16)	15	1	Sn[b] = 0.81, Sp[c] = 0.93, PPV[d] = 0.92,
Stable samples (16)	3	13	NPV[e] = 0.83, ACC[f] = 0.87, KC[g] = 0.75

[a] Dual Energy CT.
[b] Sensitivity.
[c] Specificity.
[d] Positive predictive value.
[e] Negative predictive value.
[f] Accuracy.
[g] Kappa coefficient.

3.4. Scanning Electron Microscope-Energy Dispersive X-ray Spectroscopy Analysis

SEM-EDS investigation reveals greater details about the elemental composition of samples. SEM images (Fig. 5) illustrates typical plaque surfaces (which may be vulnerable or stable). The plaque has layered structure, that is, what forms on the surface layer, is maintained in internal layers too after more layer are deposited on the surface. Thus, the composition found on the surface is also representative of what exists in the layers inside. EDS showed plaque has a highly porous top surface because of which its density and hence electron density would be low. EDS gives results in terms of weight percent (Wt%) of various elements and does not yields any information regarding numeric value of density. Our DECT algorithm calculated the electron density (ρ_e) of these plaque which were in the range 3–4 $\times 10^{-23}$ cm^3. Independent verification of the density of the plaque is the subject of our forthcoming paper.

Fig. 6 illustrates the EDS results. The EDS analysis revealed presence of low atomic number(Z) elements such as Carbon, Oxygen, Nitrogen (N) and also high Z or heavy elements like Fluorine (F), Sodium (Na), Magnesium (Mg), Silicon (Si), Phosphorus (P), Sulphur (S), Chloride (Cl), Potassium (K) and calcium (Ca) in plaque. Now, sample to sample correspondence between EDS and gold standard pathology revealed weight percent (wt%) of Nitrogen in stable and vulnerable plaque to be 11.9 (± 4.6) and 2.3% (± 1.8) wt% respectively. Similarly, heavy element's combined average wt% was found to be of 3.81(± 1.7) and of 5.7(± 1.7) wt% in stable and vulnerable plaques respectively.

Composition of vulnerable and stable plaque was statistically different (student *t*-test at $p < .05$) as tabulated in Table 2. It can be seen from Fig. 6(a & b) that elements are widely separated into two samples, namely the stable plaque and vulnerable plaque for the weight percentages of (a) Nitrogen and (b) Heavy elements. In order to test the acceptability of the hypothesis that the two samples belong to same population, we subject the hypothesis to student's *t* test. The results are shown in Table 2. It can be seen that for all cases, $t > 2.042$ which is the critical value of t for $p < .05$. Hence the above hypothesis can be rejected with 95% confidence.

Threshold value of Nitrogen was computed to be below 6.1 wt% for vulnerable plaque with AUC: 0.94 (95% CI: 0.84–1.03) as shown in Fig. 7a. Similarly, high Z elements above 4.4 wt% for vulnerable plaque with AUC: 0.80 (95% CI: 0.64–0.97) as shown in Fig. 7b.

Based on these threshold values each sample was differentiated into vulnerable or stable plaque by SEM-EDS. The results of each samples obtained from EDS were compared with pathology. 22 samples were identified as vulnerable while 10 samples were found to be stable. Table 3 reports the statistical analysis of results. The level of accuracy was found to be satisfactory and thus, the reliability of EDS was established.

The average content of all the elements like carbon, oxygen, nitrogen and heavy elements were reported in Table 2. These results were used to explain DECT findings. From EDS results we can figure out that vulnerable plaques have relatively higher wt% of high Z elements (Fig. 6) and lower wt% of nitrogen. Simultaneously, DECT establishes that vulnerable plaque has lower number of data points (Fig. 4) in region I i.e., low Z_{eff} region (< 7.4) and higher number of data points (Fig. 4) in region II, i.e., high Z_{eff} region (> 7.4) as compared to the stable plaques. Hence, from the results of DECT and EDS we conclude that stable plaques largely lie in region I, due to their higher wt% of nitrogen, while vulnerable plaques lie in region II of scatter diagram. Since, they contain a large wt% of high Z elements. The phenomenon behind these observations has been explained in discussions.

4. Discussions

This study investigates the utility of DECT as a non-invasive tool to identify the nature of non-calcified plaque as vulnerable or stable. This paper uses material (plaque) specific and machine independent parameters (Z_{eff} and ρ_e) to determine the nature of plaque. This made our process of characterization reliable, accurate and more sensitive compared to other methods [6–10,12–15,20]. This paper accurately predicts the nature of non-calcified plaque as vulnerable or stable which has hitherto remained poorly achieved with CT in the existing literature. The EDS analysis identifies the chemical components in each

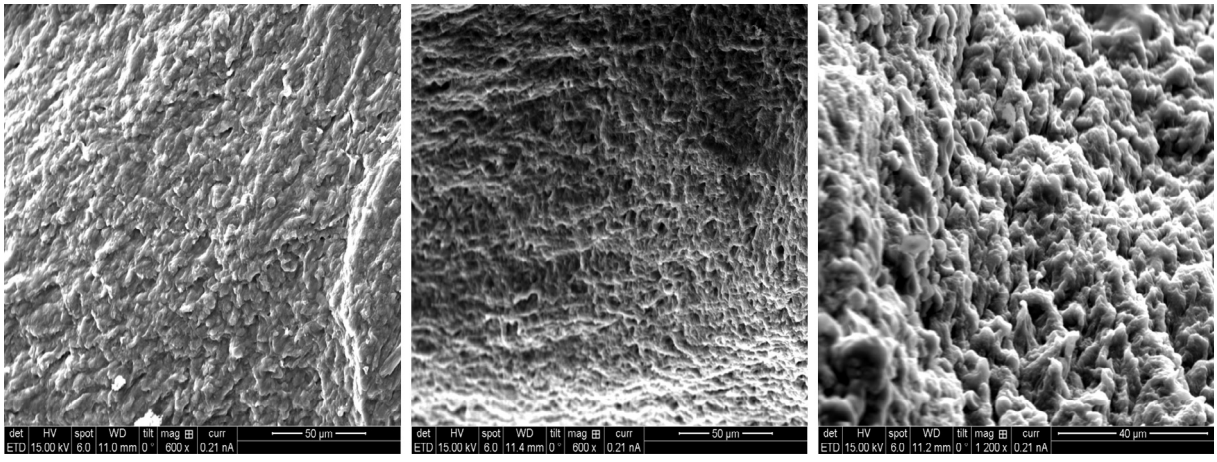

Fig. 5. Scanning electron micrographs of typical plaque's surface showing highly porous and layered structure.

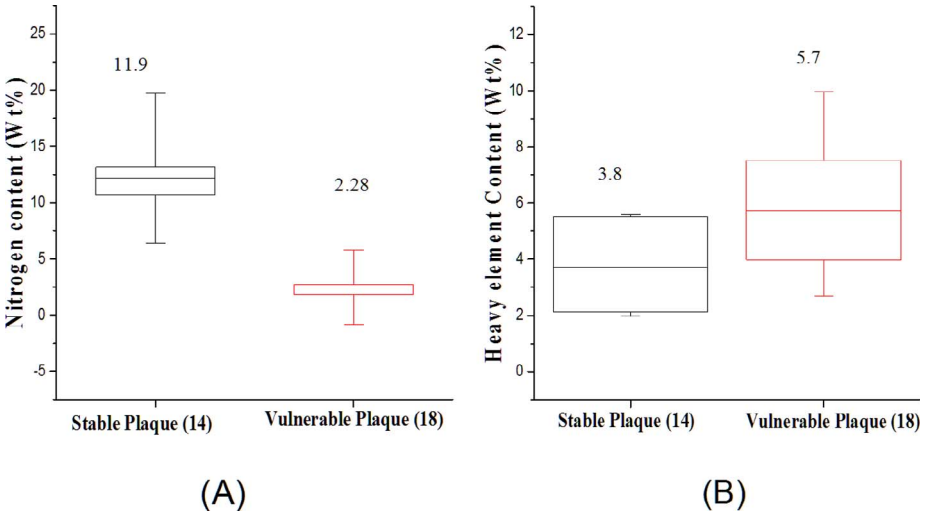

Fig. 6. Weight % (mean ± std) by EDS (a) Nitrogen, (b) Heavy Elements in pathological vulnerable and stable plaque.

Table 2
Student's *t* test calculation for discrimination between atomic weight percentage data of stable and vulnerable plaque.

Elements	Stable plaque (Sample size = 14)		Vulnerable plaque (Sample size = 16)		t value
	Sample mean (m_1)	Standard deviation (s_1)	Sample mean (m_2)	standard deviation (s_2)	
Nitrogen	11.9	4.6	2.28	1.8	8.21
Heavy elements	3.8	1.7	5.7	1.7	4.76

For degree of freedom = 30, and significance p > .05, the critical t is 2.042

Table 3
Comparison of results of pathology and EDS and corresponding statistical results of correlation (total number of samples = 32).

EDS[a] based differentiation	Pathology based differentiation		Statistical results of correlation
	Vulnerable samples (18)	Stable samples (14)	
Vulnerable samples (22)	18	4	Sn[b] = 1, Sp[c] = 0.71, PPV[d] = 0.81, NPV[e] = 1, ACC[f] = 0.87, KC[g] = 0.74
Stable samples (10)	0	10	

[a] Energy Dispersive X-ray Spectroscopy.
[b] Sensitivity.
[c] Specificity.
[d] Positive predictive value.
[e] Negative predictive value.
[f] Accuracy.
[g] Kappa coefficient.

plaque sample and SEM gives the morphological view of the plaque. These results were used to explain DECT outcomes.

By comparing DECT result to pathology relative higher concentration of data points (Z_{eff}, ρ_e) was found in region I for stable plaque as compared to vulnerable plaques (shown in Fig. 4a and b). Researchers have stated that lipid core is an unstabilizing while thick fibrous cap is a stabilizing feature for a plaque [4,5]. Therefore, logical conclusions can be drawn from before mentioned analysis to suggest that DI values may be related to the nature of plaque. It has explained as follows.

Interpretation of these DECT findings were done by EDS analysis which revealed 51% relative increase in wt% of high Z elements (such as Ca, Na, Cl, Mg, S, Si, F, K and P) in case of vulnerable plaque. Few investigations [23,24] have confirmed the presence of high Z elements along with calcium in plaques. Furthermore, calcium in plaque is most often associated with lipid burden in plaque [23–25]. Calcium salts like calcium phosphate acts as a site for crystallization of cholesterol [25].

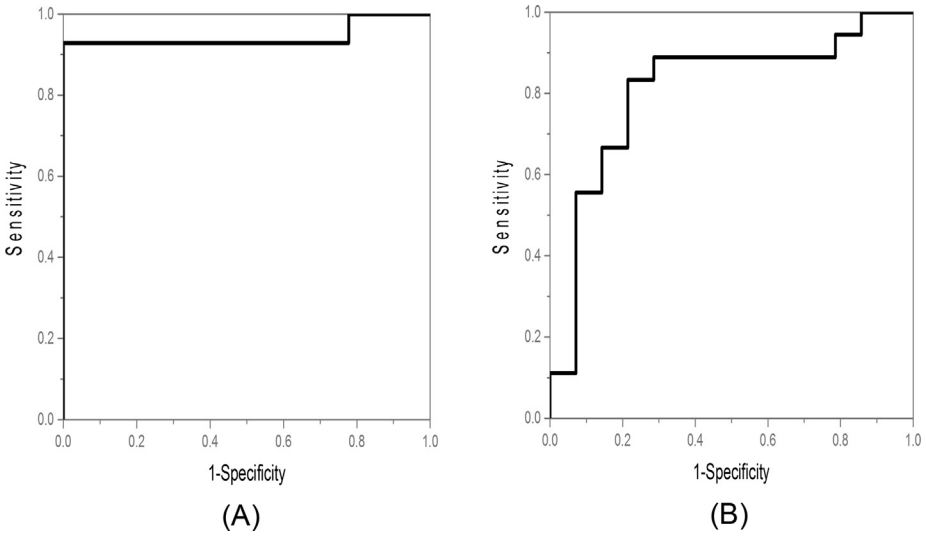

Fig. 7. (a) ROC curve for Nitrogen content of plaque (AUC 0.94, 95% CI 0.84–1.03). (b) ROC curve for Heavy elemental content of plaque (AUC 0.80, 95% CI 0.64–0.97).

Therefore, it may be fair to conclude that vulnerable plaques which are mainly the lipid-rich ones have the affinity to acquire high Z elements and a relative increase in wt% of the high Z elements element indicates the marginally higher presence of lipid in plaque. This increased presence of high Z elements leads to lower value of DI in vulnerable plaque. However, the presence of large amount of lipid doesn't alone makes a plaque vulnerable. The thickness of the fibrous cap is considered as the most crucial determinant of vulnerability [2,4,5]. In our work EDS also showed 81% relative decrease in wt% of nitrogen in vulnerable plaques with respect to stable ones which may be correlated with the leaner fibre content. Lipids and waxes are made of chains of fatty acid [26], whereas, fibres are made up of proteins which are chains of amino acids linked by peptide bonds [26]. Amino acids consists of amine (–NH2) and carboxylic group (–COOH) whereas, the fatty acid consists of chains of (–COOH) only. Hence the increased presence of nitrogen as observed by EDS may be taken as a sign of the fibrous part of the plaque. This higher nitrogen content in the plaque lead to higher DI values in stable plaque. ROC analysis of EDS results gave threshold value of nitrogen below 6.1 wt% and high Z elements above 4.4 wt% for a vulnerable plaque. These features are the hallmarks of vulnerable plaque have been lucidly brought out by EDS study.

The higher Z_{eff} for vulnerable plaque than stable plaque could be explained by the relative higher presence of high Z elements in trace amount in plaque and was found to be statistically significant at $p < .05$. This has caused Z_{eff} of vulnerable plaque to be more than that of stable. This essentially means that the non-calcified plaque has high Z elements trapped in them and more so in vulnerable plaque. This feature cannot be seen in DECT images, or by histopathology but found by DECT inversion and now is conclusively confirmed by EDS analysis. This confirmation has provided strong support to our DECT inversion algorithm.

This presence of high Z_{eff} material was also concluded in our previous work [18] purely on the basis of the physics of bonding between protein and lipid with high Z_{eff} materials, particularly calcium. It was noted in that papers that more confirmatory evidence, other than histopathology, was needed to confirm these conclusions directly. EDS studies of plaque and its correlation with histopathology and DECT analysis in the present paper confirms the same.

5. Conclusions

The study confirms the correctness of the Z_{eff} values, as given by DECT inversion method with the help of an independent elemental composition data obtained from EDS study. This supports assertion that non-calcified plaques have high Z elements metal rich components, which are undetectable by conventional histopathology methods but are revealed by DECT inversion. The present paper reveals further finer details of morphology and chemical constituent of non-calcified coronary artery plaque. The present paper proves the utility of DECT to discriminate vulnerable and stable plaque non-invasively and has provided a new method for non-invasive characterization of nature of non-calcified coronary artery plaque. The experiments were carried out in a tertiary care hospital with 52 samples collected from male and only 3 samples were collected from female during Postmortem. The whole work has been carried out in ex-vivo samples of excised coronary artery and hence attempts must be made to check its applicability in patients.

Acknowledgement

The author wishes to express her thanks to her colleagues, staff members of AIIMS mortuary and department of Cardiac-Biochemistry.

Funding

This work was funded by the Indian council of Medical Research [5/20-8(Bio)/09- NCD-I].

Competing interests

None declared.

Appendix A. Supplementary data

Supplementary data associated with this article can be found, in the online version, at http://dx.doi.org/10.1016/j.ejmp.2017.12.006.

References

[1] Berliner JA, Navab M, Fogelman AM, et al. Atherosclerosis: basic mechanisms oxidation, inflammation, and genetics. Circulation 1995;91:2488–96.
[2] Finn AV, Nakano M, Narula J, et al. Concept of vulnerable/unstable plaque. Arterioscler Thromb Vasc Biol 2010;30:1282–92.
[3] Ouhlous M, Flach HZ, de Weert TT, et al. Carotid plaque composition and cerebral infarction: MR imaging study. AJNR Am J Neuroradiol 2005;26:1044–9.
[4] Fayad ZA, Fuster V. Clinical imaging of the high-risk or vulnerable atherosclerotic plaque. Circ Res 2001;89:305–16.
[5] Loree HM, Kamm RD, Stringfellow RG, et al. Effects of fibrous cap thickness on peak circumferential stress in model atherosclerotic vessels. Circ Res 1992;71:850–8.
[6] Motoyama S, Ito H, Sarai M, et al. Plaque characterization by coronary computed tomography angiography and the likelihood of acute coronary events in mid-term follow-up. J Am Coll Cardiol 2015;66:337–46.
[7] Hoffmann U, Moselewski F, Nieman K, et al. Noninvasive assessment of plaque morphology and composition in culprit and stable lesions in acute coronary syndrome and stable lesions in stable angina by multidetector computed tomography. J Am Coll Cardiol 2006;47:1655–62.
[8] Achenbach S, Moselewski F, Ropers D, et al. Detection of calcified and noncalcified coronary atherosclerotic plaque by contrast-enhanced, submillimeter multidetector spiral computed tomography a segment-based comparison with intravascular ultrasound. Circulation 2004;109:14–7.
[9] Barreto M, Schoenhagen P, Nair A, et al. Potential of dual-energy computed tomography to characterize atherosclerotic plaque: ex vivo assessment of human coronary arteries in comparison to histology. J Cardiovasc Comput Tomogr 2008;2:234–42.
[10] Hur J, Kim YJ, Lee HJ, et al. Quantification and characterization of obstructive coronary plaques using 64-slice computed tomography: a comparison with intravascular ultrasound. J Comput Assist Tomogr 2009;33:186–92.
[11] Kataoka Y, Puri R, Hammadah M, et al. Spotty calcification and plaque vulnerability in vivo: frequency-domain optical coherence tomography analysis. Cardiovasc Diagn Ther 2014;12(4):460–9.
[12] Leber AW, Becker A, Knez A, et al. Accuracy of 64-slice computed tomography to classify and quantify plaque volumes in the proximal coronary system: a comparative study using intravascular ultrasound. J Am Coll Cardiol 2006;47:672–7.
[13] Henzler T, Porubsky S, Kayed H, et al. Attenuation-based characterization of coronary atherosclerotic plaque: comparison of dual source and dual energy CT with single-source CT and histopathology. Eur J Radiol 2011;80:54–9.
[14] Saito M. Potential of dual-energy subtraction for converting CT numbers to electron density based on a single linear relationship. Med Phys 2012;39:2021–30.
[15] Obaid DR, Calvert PA, Gopalan D, et al. Dual-energy computed tomography imaging to determine atherosclerotic plaque composition: a prospective study with tissue validation. J Cardiovasc Comput Tomogr 2014;8:230–7.
[16] Funama Yoshinori, Utsunomiya Daisuke, Oda Seitaro, Shimonobo Toshiaki, Nakaura Takeshi, Mukunoki Toshifumi, et al. Transluminal attenuation-gradient coronary CT angiography on a 320-MDCT volume scanner: effect of scan timing, coronary artery stenosis, and cardiac output using a contrast medium flow phantom. Phys Med 2016;32(11):1415–21.
[17] Haghighi RR, Chatterjee S, Vyas A, et al. X-ray attenuation coefficient of mixtures: inputs for dual-energy CT. Med Phys 2011;38:5270–9.
[18] Haghighi RR, Chatterjee S, Tabin M, et al. DECT evaluation of noncalcified coronary artery plaque. Med Phys 2015;42:5945–54.
[19] Shimomura Kohei, Araki Fujio, Kono Yuki, Asai Yoshiyuki, Murakami Takamichi, Hyodo Tomoko, et al. Identification of elemental weight fraction and mass density of humanoid tissue-equivalent materials using dual energy computed tomography. Phys Med 2017. http://dx.doi.org/10.1016/j.ejmp.2017.05.060. (in press).
[20] Becker CR, Nikolaou K, Muders M, et al. Ex vivo coronary atherosclerotic plaque characterization with multi-detector-row CT. Eur Radiol 2003;13:2094–8.
[21] Patri A, Umbreit T, Zheng J, et al. Energy dispersive X-ray analysis of titanium dioxide nanoparticle distribution after intravenous and subcutaneous injection in mice. J Appl Toxicol 2009;29:662–72.
[22] McNeil BJ, Hanley JA. Statistical approaches to the analysis of receiver operating characteristic (ROC) curves. Med Decis Making 1983;4:137–50.
[23] Balakrishnan KR, Kuruvilla S, Srinivasan A, et al. Electron microscopic insights into the vascular biology of atherosclerosis study of coronary endarterectomy specimens. Circulation 2007;115:e388–90.
[24] Srinivasan A, Ramaswamy V, Kuruvilla S, et al. Calcified atherosclerotic plaque-where exactly is the calcium and what does it contain? Indian J Thorac Cardiovasc Surg 2012;28:6–14.
[25] Van den Berg AA, Van Buul JD, Tytgat GN, Groen AK, Ostrow JD. Mucins and calcium phosphate precipitates additively stimulate cholesterol crystallization. J Lipid Res 1998;39:1744–51.
[26] Manohara SR, Hanagodimath SM, Gerward L. The effective atomic numbers of some biomolecules calculated by two methods: a comparative study. Med Phys 2009;36:137–41.